Research Square

Preprints are preliminary reports that have not undergone peer review.
They should not be considered conclusive, used to inform clinical practice,
or referenced by the media as validated information.

Conditioned medium from the stem cells of human exfoliated deciduous teeth ameliorates neuropathic pain in a partial sciatic nerve ligation model

Yao Liu
University of Tokushima: Tokushima Daigaku
Fumiya Kano (fkano@tokushima-u.ac.jp)
University of Tokushima: Tokushima Daigaku
Noboru Hashimoto
University of Tokushima: Tokushima Daigaku
Linze Xia
University of Tokushima: Tokushima Daigaku
Hideharu Hibi
Nagoya University: Nagoya Daigaku
Tsutomu Iwamoto
Tokyo Medical and Dental University: Tokyo Ika Shika Daigaku
Yoshizo Matsuka
University of Tokushima: Tokushima Daigaku
Eiji Tanaka
University of Tokushima: Tokushima Daigaku
Akihito Yamamoto
University of Tokushima: Tokushima Daigaku

Research

Keywords: Neuropathic pain, Dental pulp stem cells, Macrophages, MCP-1, Siglec-9, Conditioned medium

Posted Date: March 2nd, 2021

DOI: https://doi.org/10.21203/rs.3.rs-279355/v1

License: This work is licensed under a Creative Commons Attribution 4.0 International License.
Read Full License

Version of Record: A version of this preprint was published at Frontiers in Pharmacology on March 31st, 2022. See the published version at https://doi.org/10.3389/fphar.2022.745020.

Abstract

Background

Although recent studies have revealed the powerful antinociceptive effect of human dental pulp stem cells in an animal model for diabetes and osteoarthritis, its analgesic mechanisms are still largely elusive. We have previously reported that conditioned medium (CM) from dental pulp stem cells of deciduous teeth (SHED-CM) or its components, monocyte chemoattractant protein-1 (MCP-1) and the secreted ectodomain of sialic acid-binding Ig-like lectin-9 (sSiglec-9), directly induces anti-inflammatory M2 macrophages, however the antinociceptive activity of induced M2 is unknown. In this study, we investigated the antinociceptive effect of SHED-CM, MCP-1, and sSiglec-9 or secretome from M2-induced by SHED-CM (M2-CM) against neuropathic pain (NP) using a partial sciatic nerve ligation (PSL) mouse model and analyzed the mechanical bases of their antinociceptive effects.

Methods

PSL mice were treated using SHED-CM with or without mannosylated-Clodrosome, specifically depleting M2 macrophages, recombinant MCP-1 and sSiglec-9 protein, M2-CM, or fibroblast-CM. Human Schwann cells activated by TNF-α *in vitro* were treated with M2-CM. The expression of pro-inflammatory mediators, neuroprotective factors, the nociceptive receptor, and markers for M1, M2, and activated glial cells in injured sciatic nerve (SCN), dorsal root ganglion, or spinal cord were evaluated by RT-PCR and immunohistochemistry. Mechanical allodynia of PSL mice was analyzed via von Frey test.

Results

In the behavioral test, intravenous administration of SHED-CM greatly improved the PSL-induced hypersensitivity. SHED-CM treatment recruited M2 macrophages in the injured SCN and ipsilateral L4/L5 dorsal root ganglion and suppressed microglial activation in the spinal cord. Specific depletion of the M2 by mannosylated-Clodrosome markedly reduced the antinociceptive effect of SHED-CM. Intravenous administration of both MCP-1/sSiglec-9 and M2-CM ameliorated the PSL-induced hypersensitivity. We found that M2-CM directly suppressed the expression of nociceptive receptors as well as proinflammatory mediators in Schwann cells.

Conclusion

Taken together, our data suggest that SHED-CM ameliorates NP through the induction of the analgesic anti-inflammatory M2 macrophages. Thus, SHED-CM may present as a potential novel therapeutic candidate for NP.

Methods

Animals

All animal experiments were approved by the Animal Research Committees of Tokushima University and conformed to the ethical guidelines of the International Association for the Study of Pain (39) and ARRIVE. Male ICR mice (Charles River, Yokohama, Japan) aged 7–11 weeks were used in all the experiments. All the mice were housed in plastic cages under standard laboratory conditions (12-hour dark/light cycle, temperature controlled between 23 and 24°C) and provided with water and food *ad libitum*. An overview of the experimental design and workflow is presented in Additional file 1.

Results

SHED-CM prevents the partial sciatic nerve ligation-induced pain

We tightly ligated 1/3 to 1/2 of the SCN on the right side in mice to induce NP. A decrease in the threshold for tactile stimuli was observed after nerve ligation. The threshold was reached in a minimum of 3 days after PSL and was maintained at the level for weeks. Daily intravenous administration of SHED-CM, immediately after PSL, inhibited PSL-induced mechanical allodynia (Figs. 1a and b; early phase). These antinociceptive effects of SHED-CM were detected even 3 days after the administration of SHED-CM. In the von Frey test, the threshold for the right hindpaw at day 3 was 6.73 ± 1.5 g in the SHED-CM group and 4.28 ± 1.48 g in the DMEM group. On day 7, the threshold of SHED-CM group was 8.39 ± 0.99 g, which was significantly higher than 4.29 ± 1.77 g in the DMEM group. In contrast, no antinociceptive effects were observed in the Fibro-CM group (Fig. 1b). We also examined whether SHED-CM could attenuate PSL-induced pain in a well-developed phase (middle phase). SHED-CM treatment exhibited significant antinociceptive effects in the middle phase model, in which the threshold of the SHED-CM group was 8.07 ± 0.84 g and of the DMEM group was 4.82 ± 0.92 g at 14 days after PSL (Figs. 1c and d). In the late phase, the threshold of the SHED-CM group was 9.47 ± 0.74 g and that of the DMEM group was 5.07 ± 0.67 g at 21 days after PSL (Figs. 1e and f). During the SHED-CM treatment, the von Frey test data of the contralateral side did not show any change (Additional file 3: Suppl. Figure 2). None of the test groups showed signs of motor weakness during the experimental period.

Results

SHED-CM prevents the partial sciatic nerve ligation-induced pain

We tightly ligated 1/3 to 1/2 of the SCN on the right side in mice to induce NP. A decrease in the threshold for tactile stimuli was observed after nerve ligation. The threshold was reached in a minimum of 3 days after PSL and was maintained at the level for weeks. Daily intravenous administration of SHED-CM, immediately after PSL, inhibited PSL-induced mechanical allodynia (Figs. 1a and b; early phase). These antinociceptive effects of SHED-CM were detected even 3 days after the administration of SHED-CM. In the von Frey test, the threshold for the right hindpaw at day 3 was 6.73 ± 1.5 g in the SHED-CM group and 4.28 ± 1.48 g in the DMEM group. On day 7, the threshold of SHED-CM group was 8.39 ± 0.99 g, which was significantly higher than 4.29 ± 1.77 g in the DMEM group. In contrast, no antinociceptive effects

were observed in the Fibro-CM group (Fig. 1b). We also examined whether SHED-CM could attenuate PSL-induced pain in a well-developed phase (middle phase). SHED-CM treatment exhibited significant antinociceptive effects in the middle phase model, in which the threshold of the SHED-CM group was 8.07 ± 0.84 g and of the DMEM group was 4.82 ± 0.92 g at 14 days after PSL (Figs. 1c and d). In the late phase, the threshold of the SHED-CM group was 9.47 ± 0.74 g and that of the DMEM group was 5.07 ± 0.67 g at 21 days after PSL (Figs. 1e and f). During the SHED-CM treatment, the von Frey test data of the contralateral side did not show any change (Additional file 3: Suppl. Fig 2). None of the test groups showed signs of motor weakness during the experimental period.

SHED-CM treatment induces M2-polarized macrophages in PSL

To investigate the analgesic mechanism of SHED-CM, we examined the mRNA expression profiles of genes involved in pro- and anti-inflammatory responses in the early phase PSL. Seven days after PSL, the expression of inflammatory genes, TNF-α, IL-1β, and inducible nitric oxide synthase (iNOS), was greatly increased, but was markedly suppressed by the SHED-CM treatment. In contrast, the SHED-CM treatment increased the expression of pan macrophage markers, F4/80 and M2-specific molecules, CD206, arginase-1 (Arg-1), and Ym-1. Notably, we found that the SHED-CM treatment elevated the expression of an array of neurotrophic and immunosuppressive factors, brain-derived neurotrophic factor (BDNF), nerve growth factor (NGF), glial cell derived neurotrophic factor (GDNF), and transforming growth factor-β1 (TGF-β1) (Fig. 2). These results show that the SHED-CM treatment converted the proinflammatory microenvironment of PSL to anti-inflammatory and tissue-protective one.

Immunohistochemical analysis revealed that the number of $CD206^+$ $F4/80^+$ macrophages was significantly increased, but $TNF\text{-}\alpha^+$ $S100^+$ proinflammatory SCs were reduced by the SHED-CM treatment (Figs. 3a-d).

SHED-CM treatment induces M2-polarized macrophages in ipsilateral DRG

Immunohistochemical analysis of the ipsilateral L4/L5 DRG, 7 days after PSL, revealed that the SHED-CM treatment significantly increased the number of $CD206^+$ $F4/80^+$ M2 macrophages compared with the DMEM control treatment (Fig. 3e). The cell count analysis showed that the number of M2 cells in the SHED-CM group was significantly higher than that in the DMEM group (Fig. 3f), indicating that M2 not only accumulated in the ipsilateral SCN, but also in the ipsilateral DRG.

SHED-CM attenuates PSL-induced microglial activation in the spinal cord

Next, we examined microglial activation, 7 days after PSL. As shown in Fig. 3g, a substantial increase in the number of $Iba1^+$ microglia in the L3/4 ipsilateral dorsal horn was obvious compared with that in the contralateral horn. Microglial morphology in the ipsilateral side showed activated morphology with a hypertrophied soma and thicker and retracted processes, whereas that of the contralateral side seemed to be at the quiescent stage with smaller soma and ramified processes; the two kinds of morphologies are very distinguishable (43). Notably, in the SHED-CM-treated group, the number of $Iba1^+$ microglia on the

ipsilateral side was reduced, and their morphologies were very similar to those on the contralateral side (Fig. 3h). These results demonstrate that SHED-CM treatment suppressed the PSL-induced microglial activation in the spinal cord.

M2 macrophages induced by SHED-CM are required for its anti-nociceptive activity

Next, we investigated the roles of M2 macrophages in the antinociceptive activity of SHED-CM by specifically depleting them with m-Clo. After PSL, SHED-CM was injected daily for 7 consecutive days, and from day 4 to day 6, m-Clo or m-Enc was injected together with SHED-CM (Fig. 4a).

The antinociceptive effects were similar in both the groups at day 3; however, m-Clo, but not m-Enc, significantly decreased at day 5. On day 7, the von Frey test of the m-Clo, m-Enc, and DMEM groups was 5.49 ± 0.92 g, 7.9 ± 1.33 g, and 4.57 ± 1.00 g, respectively (Fig. 4b). None of the test groups showed signs of motor weakness during the experimental period.

Immunohistochemical analysis showed that m-Clo, but not m-Enc, reduced the number of $CD206^+$ $F4/80^+$ macrophages in SCN and DRG, while increasing $TNF\text{-}\alpha^+$ $S100^+$ proinflammatory SCs in SCN and $Iba1^+$ activated microglia in the spinal cord (Figs. 5a-h). These results show that SHED-CM-induced M2 macrophages are crucial for the suppression of proinflammatory response and antinociceptive activity.

CM from M2 induced by SHED-CM suppressed proinflammatory activities of Schwann cells in vitro

We next examined the biological activity of the secretion from M2 induced by SHED-CM. MCSF-treated bone marrow cells differentiated into macrophages, which were subsequently stimulated with SHED-CM for 24 h. Using this procedure, more than 68.48% of the cells differentiated into $CD206^+F4/80^+$M2 macrophages (Fig. 6a). We harvested the secretion from M2 induced by SHED-CM as M2-CM.

SCs first detect nerve injury and play a critical role in the development and maintenance of NP. Under proinflammatory conditions, they express cytokines TNF-α and IL-1β, chemokine MCP-1, and transient receptor potential ankyrin 1 (TRPA 1) channels, which accelerate neuroinflammation and mechanical allodynia. We treated human SCs with TNF-α or M2-CM for 24 h and analyzed the gene expression profile. The TNF-α treatment increased the expression of TRPA1, TNF-α, IL-1β, and MCP-1, whereas the M2-CM treatment strongly suppressed this upregulation (Fig. 6b).

SHED-CM derived M2-CM attenuates neuropathic pain in vivo

To examine the antinociceptive activity of M2-CM, we administered it to the PSL mice. We found that M2-CM, but not DMEM, prevented PSL-induced allodynia and proinflammatory responses in the SCN (Figs. 7a-c). On the ipsilateral side of L3/4, $IBA1^+$ positive cells were extensively decreased in the M2-CM group compared with that in the DMEM group (Figs. 7d and e). Taken together, these results suggest that SHED-CM suppressed the neuroinflammation and mechanical allodynia in part through the analgesic effect of M2.

The therapeutic factors in SHED-CM attenuate neuropathic pain in vivo

To confirm the therapeutic effects of a set of M2 inducers, MCP-1 and sSiglec-9, in SHED-CM, we intravenously administered them to the PSL mice. We found that, in the middle phase setting, the von Frey test of the right hindpaw of the MCP-1/sSiglec-9 group at day 14 was 7.32 ± 1.75 g, which was significantly higher than that of the DMEM and PBS groups but was lower than that of the SHED-CM group (Figs. 7f and g). These results suggest that the promising analgesic ability of SHED-CM may partly rely on MCP-1/sSiglec-9.

Discussion

Here, we report the potential of SHED-CM for the treatment of NP. Intravenous administration of SHED-CM in the early, middle, and late phases of PSL mice prevented nociceptive responses. The qPCR and immunostaining analysis revealed that SHED-CM treatment induced anti-inflammatory M2 macrophages in injured SCN and DRG, and suppressed the PSL-induced pro-inflammatory conditions in SCN and microglial activation in SCs. Importantly, the specific depletion of M2 induced by SHED-CM negated its analgesic effect. Furthermore, our data show that the secretome from M2 directly inhibited the proinflammatory/pain-inducing property of SCs and restored NP after PSL. Taken together, our data suggest that the SHED-CM treatment prevented NP mainly through the induction of the analgesic M2.

M2 has been considered to play a crucial role in ameliorating NP(44). However, the detailed mechanisms by which M2 inhibits pain have only been investigated in a few studies. It has been reported that perineural injection of IL-4 resulted in the recruitment of M2 in the SCN in the PSL model, which exhibited an analgesic effect by inhibiting the expression of proinflammatory cytokines and chemokines in the injured SCN (14). In a recent study, it was shown that IL-4-induced M2 produced opioid peptides, which activated the peripheral opioid receptors and, thereby, ameliorated pain (15). We found that the M2-CM treatment directly suppressed the expression of TRPA1 as well as of proinflammatory cytokines and chemokines in TNF-α-activated human SCs and effectively inhibited PSL-induced pain. To our knowledge, this is the first study to demonstrate the analgesic effect of M2-CM. It was recently reported that TRPA1 in SCs contributes to NP by evoking the NADPH oxidase 1-dependent H_2O_2 release. TRPA1 silencing in SCs attenuated nerve injury-induced allodynia and neuroinflammation (45). Thus, based on our findings, we suggest that, in addition to the previously reported analgesic mechanisms of M2, the direct action of M2 against the proinflammatory/pain-inducing property of SCs may play a significant role in the multifaceted analgesic actions of M2.

In our previous studies, we identified a set of M2 inducers, sSiglec-9 and MCP-1, by secretome analysis of SHED-CM. Neither MCP-1 nor sSiglec-9 alone could recapitulate the M2-inducing activity of SHED-CM. The combination of MCP-1 and sSiglec-9 recapitulated the SHED-CM activity for the induction of M2-like macrophages. In this study, we found that the antinociceptive activity of the MCP-1/sSiglec-9 treatment was significantly inferior to that of SHED-CM. Even after M2 depletion, the threshold for tactile stimuli of the m-Clo group was significantly better than that of the DMEM group. These data raise the possibility

that SHED-CM is composed of anti-pain factors other than MCP-1/sSiglec-9. In a previous study (33), we characterized the soluble factors in SHED-CM by performing an LC-MS/MS analysis and found that SHED-CM contained 51 of the array proteins at levels more than 10-fold higher than those detected in fibroblast-CM. It was reported that secreted frizzled-related protein 1 (SFRP1), a Wnt antagonist, is a therapeutic agent for NP because of its anti-inflammatory activity (46). TGF-β inhibits the expression of proinflammatory cytokines and hence suppresses the activation and proliferation of glial cells in the spinal cord in a mouse nerve injury model (47, 48). Notably, TGF-β also suppresses nerve injury-induced spinal cord synaptic plasticity and DRG neuronal hyperexcitability (49). Recently, the effectiveness of alpha 2 macroglobulin (A2M) was investigated in the neurogenic thoracic outlet syndrome and other forms of cervical brachial syndrome. A2M is a plasma protein that acts as a molecular trap for inflammatory factors, which counteracts inflammation and hence ameliorates pain (50). Hepatocyte growth factor (HGF) shown to possess potential angiogenic and neurotrophic properties. HGF attenuates NP by suppressing pain-related genes, activating transcription factor 3 (ATF3), α2δ1, and colony stimulating factor 1 (CSF1) in DRG neurons (51). In diabetic NP, increasing glucose-6-phosphate dehydrogenase in DRGs attenuated hindpaw hypersensitivity because of suppression of toll-like receptor 4 (52). The concentrations of these factors in SHED-CM may be quite low; however, we believe that the combinatorial effects of these factors in SHED-CM may provide therapeutic benefits for treating NP. The roles of these therapeutic factors in SHED-CM-mediated analgesic effects should be investigated in the future.

Conclusions

In this study, we demonstrate the potential of SHED-CM for treating NP. Although the treatment of NP remains a clinical challenge, our results suggest that increasing M2 macrophages after the administration of SHED-CM may be a promising method to modify the microenvironment in peripheral nerves and, thereby, cure neuropathic pain.

Abbreviations

NP, neuropathic pain; CM, conditioned medium; SHED, stem cells from human exfoliated deciduous teeth; SHED-CM, conditioned medium derived from stem cells from human exfoliated deciduous teeth; M2-CM, conditioned medium derived from M2 macrophage; Fibro-CM, fibroblast-CM; DPSC, dental pulp stem cell; DMEM, Dulbecco's modified Eagle's medium; MCSF, macrophage colony stimulating factor; PSL, partial sciatic nerve ligation; SC, Schwann cell; SCN, sciatic nerve; m-Enc, mannosylated control liposome; m-Clo, mannosylated-Clodrosome; MCP-1, monocyte chemoattractant protein-1; sSiglec-9, secreted ectodomain of sialic acid-binding Ig-like lectin-9; GAPDH, glyceraldehyde-3-phosphate dehydrogenase; TNF-α, tumor necrosis factor-α; IL-1β, interleukin-1β; iNOS, inducible nitric oxide synthase; Arg-1, arginase-1; BDNF, brain-derived neurotrophic factor; NGF, nerve growth factor; GDNF, glial cell derived neurotrophic factor; TGF-β, transforming growth factor-β; TRPA1, transient receptor potential ankyrin 1; SFRP1, secreted

frizzled-related protein 1; A2M, alpha 2 macroglobulin; HGF, hepatocyte growth factor; ATF3, activating transcription factor 3; CSF1, colony stimulating factor 1.

Declarations

Ethics approval and consent to participate

This study was approved by the Institutional Ethical Committee of Nagoya University and Tokushima University Hospital and performed according to the principles of Helsinki Declaration (Permit No H-73 and No: 3268 for Nagoya and Tokushima University, respectively). All procedures performed in this study involving animals were approved by the Tokushima University Animal Care and Use Committee (Permit No: T30-95) and in accordance with the guidelines of the International Association for the Study of Pain.

Consent for publication

Not applicable.

Availability of data and materials

There is no data, software, databases, and application/tool available apart from the reported in the present study. All data is provided in manuscript.

Competing interests

The authors declare that there is no conflict of interest.

Funding

This work was supported by Grants-in-Aid for Scientific Research on Priority Areas from the Ministry of Education, Culture, Sports, Science, and Technology of Japan (22390372).

Authors' Contributions

Y.L.: Conducted all the PSL experiments and wrote the manuscript; F.K., N.H., Y.M., and LZ.X.: Provided support for the PSL experiments; H.H. and T.I .:Provided materials; F.K. and A.Y.: Designed the experiments and wrote the manuscript. Y.M., E.T., and A.Y. Supervised the project.

Acknowledgements

We thank support center of Tokushima University, Fujii Memorial Institute of Medical Sciences, for housing the mice and for microscope maintenance, respectively.

References

1. Ji RR, Xu ZZ, Gao YJ. Emerging targets in neuroinflammation-driven chronic pain. Nat Rev Drug Discov. 2014;13(7):533-48.
2. Sommer C, Leinders M, Uceyler N. Inflammation in the pathophysiology of neuropathic pain. Pain. 2018;159(3):595-602.
3. Ji RR, Chamessian A, Zhang YQ. Pain regulation by non-neuronal cells and inflammation. Science. 2016;354(6312):572-7.
4. Calvo M, Dawes JM, Bennett DL. The role of the immune system in the generation of neuropathic pain. Lancet Neurol. 2012;11(7):629-42.
5. Argoff C. Mechanisms of pain transmission and pharmacologic management. Curr Med Res Opin. 2011;27(10):2019-31.
6. Costigan M, Scholz J, Woolf CJ. Neuropathic pain: a maladaptive response of the nervous system to damage. Annu Rev Neurosci. 2009;32:1-32.
7. Guo W, Chu YX, Imai S, Yang JL, Zou SP, Mohammad Z, et al. Further observations on the behavioral and neural effects of bone marrow stromal cells in rodent pain models. Molecular Pain. 2016;12.
8. Davies LC, Jenkins SJ, Allen JE, Taylor PR. Tissue-resident macrophages. Nat Immunol. 2013;14(10):986-95.
9. Inoue K, Tsuda M. Microglia in neuropathic pain: cellular and molecular mechanisms and therapeutic potential. Nat Rev Neurosci. 2018;19(3):138-52.
10. Mantovani A, Biswas SK, Galdiero MR, Sica A, Locati M. Macrophage plasticity and polarization in tissue repair and remodelling. J Pathol. 2013;229(2):176-85.
11. Murray PJ, Allen JE, Biswas SK, Fisher EA, Gilroy DW, Goerdt S, et al. Macrophage activation and polarization: nomenclature and experimental guidelines. Immunity. 2014;41(1):14-20.
12. Murray PJ, Wynn TA. Protective and pathogenic functions of macrophage subsets. Nat Rev Immunol. 2011;11(11):723-37.
13. Gordon S, Martinez FO. Alternative activation of macrophages: mechanism and functions. Immunity. 2010;32(5):593-604.
14. Kiguchi N, Kobayashi Y, Saika F, Sakaguchi H, Maeda T, Kishioka S. Peripheral interleukin-4 ameliorates inflammatory macrophage-dependent neuropathic pain. Pain. 2015;156(4):684-93.
15. Celik MO, Labuz D, Keye J, Glauben R, Machelska H. IL-4 induces M2 macrophages to produce sustained analgesia via opioids. JCI Insight. 2020;5(4).
16. Venturi M, Boccasanta P, Lombardi B, Brambilla M, Contessini Avesani E, Vergani C. Pudendal Neuralgia: A New Option for Treatment? Preliminary Results on Feasibility and Efficacy. Pain Med. 2015;16(8):1475-81.
17. Vickers ER, Karsten E, Flood J, Lilischkis R. A preliminary report on stem cell therapy for neuropathic pain in humans. J Pain Res. 2014;7:255-63.
18. Wang Q, He H, Xie S, Wei Q, He C. Mesenchymal Stem Cells Transplantation for Neuropathic Pain Induced By Peripheral Nerve Injury in Animal Models: A Systematic Review. Stem Cells Dev.

2020;29(22):1420-8.
19. Asgharzade S, Talaei A, Farkhondeh T, Forouzanfar F. A Review on Stem Cell Therapy for Neuropathic Pain. Curr Stem Cell Res Ther. 2020;15(4):349-61.
20. Baraniak PR, McDevitt TC. Stem cell paracrine actions and tissue regeneration. Regen Med. 2010;5(1):121-43.
21. Ishikawa J, Takahashi N, Matsumoto T, Yoshioka Y, Yamamoto N, Nishikawa M, et al. Factors secreted from dental pulp stem cells show multifaceted benefits for treating experimental rheumatoid arthritis. Bone. 2016;83:210-9.
22. Matsubara K, Matsushita Y, Sakai K, Kano F, Kondo M, Noda M, et al. Secreted ectodomain of sialic acid-binding Ig-like lectin-9 and monocyte chemoattractant protein-1 promote recovery after rat spinal cord injury by altering macrophage polarity. J Neurosci. 2015;35(6):2452-64.
23. Matsushita Y, Ishigami M, Matsubara K, Kondo M, Wakayama H, Goto H, et al. Multifaceted therapeutic benefits of factors derived from stem cells from human exfoliated deciduous teeth for acute liver failure in rats. J Tissue Eng Regen Med. 2017;11(6):1888-96.
24. Mita T, Furukawa-Hibi Y, Takeuchi H, Hattori H, Yamada K, Hibi H, et al. Conditioned medium from the stem cells of human dental pulp improves cognitive function in a mouse model of Alzheimer's disease. Behav Brain Res. 2015;293:189-97.
25. Shimojima C, Takeuchi H, Jin S, Parajuli B, Hattori H, Suzumura A, et al. Conditioned Medium from the Stem Cells of Human Exfoliated Deciduous Teeth Ameliorates Experimental Autoimmune Encephalomyelitis. J Immunol. 2016;196(10):4164-71.
26. Wakayama H, Hashimoto N, Matsushita Y, Matsubara K, Yamamoto N, Hasegawa Y, et al. Factors secreted from dental pulp stem cells show multifaceted benefits for treating acute lung injury in mice. Cytotherapy. 2015;17(8):1119-29.
27. Yamagata M, Yamamoto A, Kako E, Kaneko N, Matsubara K, Sakai K, et al. Human dental pulp-derived stem cells protect against hypoxic-ischemic brain injury in neonatal mice. Stroke. 2013;44(2):551-4.
28. Yamaguchi S, Shibata R, Yamamoto N, Nishikawa M, Hibi H, Tanigawa T, et al. Dental pulp-derived stem cell conditioned medium reduces cardiac injury following ischemia-reperfusion. Sci Rep. 2015;5:16295.
29. Hirata M, Ishigami M, Matsushita Y, Ito T, Hattori H, Hibi H, et al. Multifaceted Therapeutic Benefits of Factors Derived From Dental Pulp Stem Cells for Mouse Liver Fibrosis. Stem Cells Transl Med. 2016;5(10):1416-24.
30. Makino E, Nakamura N, Miyabe M, Ito M, Kanada S, Hata M, et al. Conditioned media from dental pulp stem cells improved diabetic polyneuropathy through anti-inflammatory, neuroprotective and angiogenic actions: Cell-free regenerative medicine for diabetic polyneuropathy. J Diabetes Investig. 2019;10(5):1199-208.
31. Guimaraes ET, Cruz Gda S, Almeida TF, Souza BS, Kaneto CM, Vasconcelos JF, et al. Transplantation of stem cells obtained from murine dental pulp improves pancreatic damage, renal function, and

painful diabetic neuropathy in diabetic type 1 mouse model. Cell Transplant. 2013;22(12):2345-54.
32. Xie J, Rao N, Zhai Y, Li J, Zhao Y, Ge L, et al. Therapeutic effects of stem cells from human exfoliated deciduous teeth on diabetic peripheral neuropathy. Diabetol Metab Syndr. 2019;11:38.
33. Ogasawara N, Kano F, Hashimoto N, Mori H, Liu Y, Xia L, et al. Factors secreted from dental pulp stem cells show multifaceted benefits for treating experimental temporomandibular joint osteoarthritis. Osteoarthritis Cartilage. 2020;28(6):831-41.
34. Bachmann MF, Kopf M, Marsland BJ. Chemokines: more than just road signs. Nat Rev Immunol. 2006;6(2):159-64.
35. Crocker PR, Paulson JC, Varki A. Siglecs and their roles in the immune system. Nat Rev Immunol. 2007;7(4):255-66.
36. Kano F, Matsubara K, Ueda M, Hibi H, Yamamoto A. Secreted Ectodomain of Sialic Acid-Binding Ig-Like Lectin-9 and Monocyte Chemoattractant Protein-1 Synergistically Regenerate Transected Rat Peripheral Nerves by Altering Macrophage Polarity. Stem Cells. 2017;35(3):641-53.
37. Ito T, Ishigami M, Matsushita Y, Hirata M, Matsubara K, Ishikawa T, et al. Secreted Ectodomain of SIGLEC-9 and MCP-1 Synergistically Improve Acute Liver Failure in Rats by Altering Macrophage Polarity. Sci Rep. 2017;7:44043.
38. Ishikawa J, Kano F, Ando Y, Hibi H, Yamamoto A. Monocyte chemoattractant protein-1 and secreted ectodomain of sialic acid-binding Ig-like lectin-9 enhance bone regeneration by inducing M2 macrophages. Journal of Oral and Maxillofacial Surgery, Medicine, and Pathology. 2019;31(3):169-74.
39. Zimmermann M. Ethical guidelines for investigations of experimental pain in conscious animals. Pain. 1983;16(2):109-10.
40. Seltzer Z, Dubner R, Shir Y. A novel behavioral model of neuropathic pain disorders produced in rats by partial sciatic nerve injury. Pain. 1990;43(2):205-18.
41. Sakai K, Yamamoto A, Matsubara K, Nakamura S, Naruse M, Yamagata M, et al. Human dental pulp-derived stem cells promote locomotor recovery after complete transection of the rat spinal cord by multiple neuro-regenerative mechanisms. Journal of Clinical Investigation. 2012;122(1):80-90.
42. Chaplan SR, Bach FW, Pogrel JW, Chung JM, Yaksh TL. Quantitative assessment of tactile allodynia in the rat paw. J Neurosci Methods. 1994;53(1):55-63.
43. Old EA, Clark AK, Malcangio M. The role of glia in the spinal cord in neuropathic and inflammatory pain. Handb Exp Pharmacol. 2015;227:145-70.
44. Kiguchi N, Kobayashi D, Saika F, Matsuzaki S, Kishioka S. Pharmacological Regulation of Neuropathic Pain Driven by Inflammatory Macrophages. Int J Mol Sci. 2017;18(11).
45. De Logu F, Nassini R, Materazzi S, Carvalho Goncalves M, Nosi D, Rossi Degl'Innocenti D, et al. Schwann cell TRPA1 mediates neuroinflammation that sustains macrophage-dependent neuropathic pain in mice. Nat Commun. 2017;8(1):1887.

46. Tang J, Ji Q, Jin L, Tian M, Zhang LD, Liu XY. Secreted frizzled-related protein 1 regulates the progression of neuropathic pain in mice following spinal nerve ligation. J Cell Physiol. 2018;233(8):5815-22.
47. Chen NF, Huang SY, Chen WF, Chen CH, Lu CH, Chen CL, et al. TGF-beta1 attenuates spinal neuroinflammation and the excitatory amino acid system in rats with neuropathic pain. J Pain. 2013;14(12):1671-85.
48. Echeverry S, Shi XQ, Haw A, Liu H, Zhang ZW, Zhang J. Transforming growth factor-beta1 impairs neuropathic pain through pleiotropic effects. Mol Pain. 2009;5:16.
49. Chen G, Park CK, Xie RG, Ji RR. Intrathecal bone marrow stromal cells inhibit neuropathic pain via TGF-beta secretion. J Clin Invest. 2015;125(8):3226-40.
50. Jordan S, Iovine J, Kuhn T, Gelabert H. Neurogenic Thoracic Outlet Syndrome and other Forms of Cervical Brachial Syndrome Treated with Plasma Concentrate Enriched for Alpha 2 Macroglobulin. Pain Physician. 2020;23(2):229-33.
51. Nho B, Lee J, Lee J, Ko KR, Lee SJ, Kim S. Effective control of neuropathic pain by transient expression of hepatocyte growth factor in a mouse chronic constriction injury model. FASEB J. 2018;32(9):5119-31.
52. Sun Q, Zhang BY, Zhang PA, Hu J, Zhang HH, Xu GY. Downregulation of glucose-6-phosphate dehydrogenase contributes to diabetic neuropathic pain through upregulation of toll-like receptor 4 in rats. Mol Pain. 2019;15:1744806919838659.

Tables

Table1 primer sequence

Gene		Forward
mouse GAPDH	Forward	AACTTTGGCATTGTGGAAGG
mouse GAPDH	Reverse	GGATGCAGGGATGATGTTCT
mouse F4/80	Forward	CCAGAAGGCTCCCAAGGAT
mouse F4/80	Reverse	TCTGCTCACTTTGGAGTATCAAGT
mouse TNF-α	Forward	CCCTTTACTCTGACCCCTTTATTGT
mouse TNF-α	Reverse	TGTCCCAGCATCTTGTGTTTCT
mouse IL-1β	Forward	CCTCTGATGGGCAACCACTT
mouse IL-1β	Reverse	TGCTGCCTAATGTCCCCTTG
mouse iNOS	Forward	AGCCAAGCCCTCACCTACTTC
mouse iNOS	Reverse	GCCTCCAATCTCTGCCTATCC
mouse CD206	Forward	CAGGTGTGGGCTCAGGTAGT
mouse CD206	Reverse	TGTGGTGAGCTGAAAGGTGA
mouse Arginase-1	Forward	CTCCAAGCCAAAGTCCTTAGAG
mouse Arginase-1	Reverse	GGAGCTGTCATTAGGGACATCA
mouse Ym-1	Forward	CTCTCCAGAAGCAATCCTGAAGAC
mouse Ym-1	Reverse	GCCCAACTGGTATAGTAGCACATC
mouse BDNF	Forward	TTAATCGGCTTCACAGGAGACA
mouse BDNF	Reverse	AGAACGAACAGAAACGAAGAAGAGA
mouse NGF	Forward	ACAGACATCAAGGGCAAGGAG
mouse NGF	Reverse	GCACCCACTCTCAACAGGATT
mouse GDNF	Forward	TGCTAAAGGAAAGGGTCAGGAG
mouse GDNF	Reverse	GCTCAGATGGATAGAAGAGGAGATG
mouse TGF-β1	Forward	CCACCTGCAAGACCATCGAC
mouse TGF-β1	Reverse	CTGGCGAGCCTTAGTTTGGAC
human GAPDH	Forward	CTGGGCTACACTGAGCACC
human GAPDH	Reverse	AAGTGGTCGTTGAGGGCAATG
human TRPA1	Forward	AAGCCGTTGCGCTTCTTC
human TRPA1	Reverse	GACATTCATCCCATCTTTTGCTC

human TNF-α	Forward	GAGGCCAAGCCCTGGTATG
human TNF-α	Reverse	CGGGCCGATTGATCTCAGC
human IL-1β	Forward	CCTGTCCTGCGTGTTGAAAG
human IL-1β	Reverse	GGGAACTGGGCAGACTCAAA
human MCP-1	Forward	AGAATCACCAGCAGCAAGTGTC
human MCP-1	Reverse	CGGAGTTTGGGTTTGCTTGT

Figures

Figure 1

Intravenous administration of SHED-CM attenuates partial sciatic nerve ligation (PSL)-induced neuropathic pain. (A) Time course of SHED-CM treatment in the early phase model. (B) The ipsilateral paw withdrawal thresholds in the early phase. ANOVA with Tukey's post-hoc test (n = 9 in each group). (C) Time course of SHED-CM treatment in the middle phase model. (D) The ipsilateral paw withdrawal thresholds in the middle phase. Student's t test (n = 5 in each group). (E) Time course of SHED-CM treatment in the late phase model. (F) The ipsilateral paw withdrawal thresholds in the late phase. Student's t-test (n = 5 in each group). Data represent the mean ± SD. *** $p < 0.001$ and ****$p < 0.0001$ for the SHED-CM vs. DMEM or SHED-CM vs. Fibro-CM comparisons.

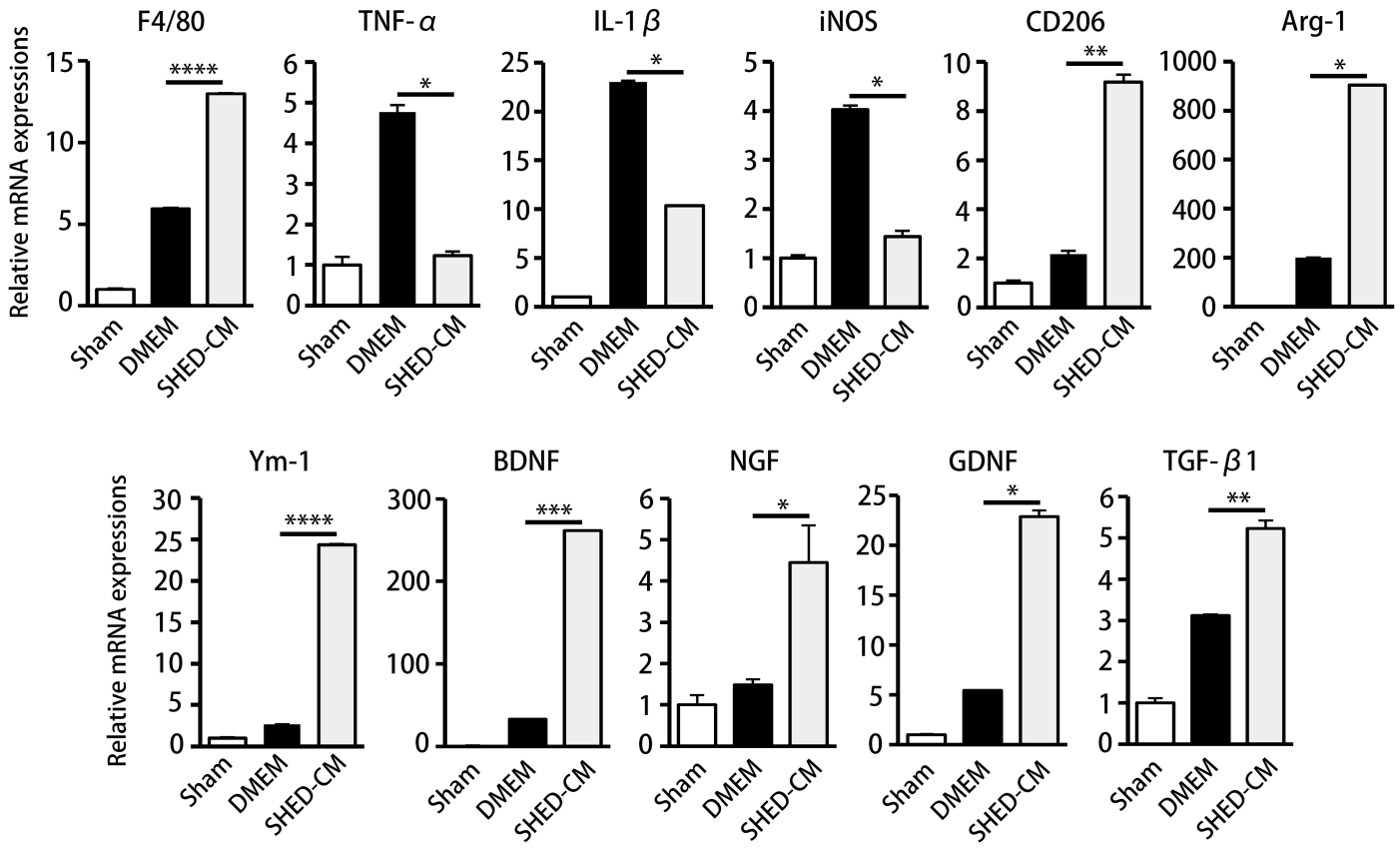


Figure 2

SHED-CM treatment converted proinflammatory microenvironment to anti-inflammatory and tissue-protective one. qPCR analysis of the indicated mRNAs in the sciatic nerves after 7 days from PSL in the early phase model. Results are expressed relative to the levels in the sham-operated model. Student's t-test (n = 3, per group). Data represent the mean ± SD. *p < 0.05, **p < 0.01, ***p < 0.001, ****p < 0.0001.

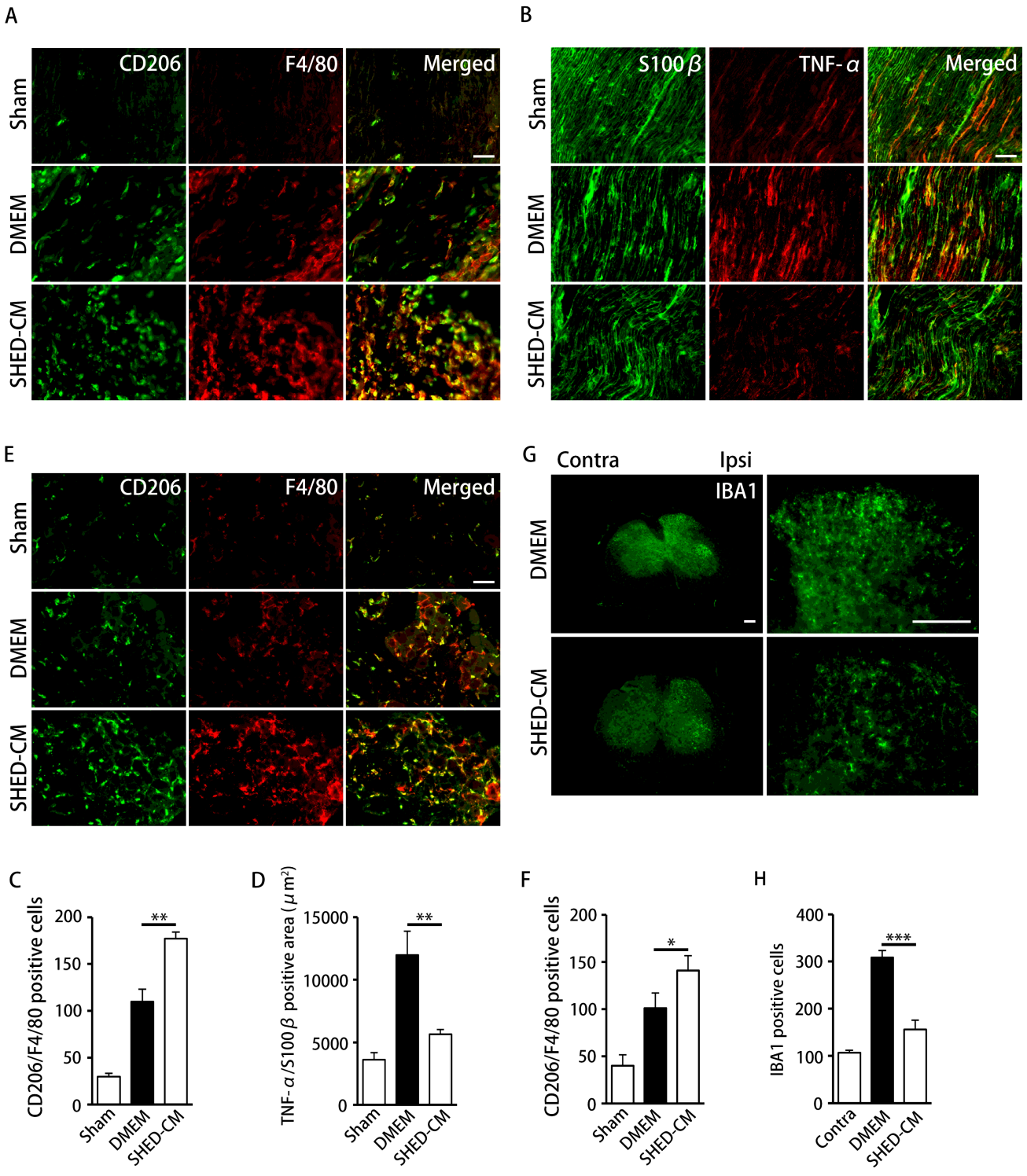


Figure 3

SHED-CM treatment induces M2 macrophages and suppresses the activation of microglia. (A, B) Representative images of immunofluorescent staining of CD206, F4/80 (A) and TNF-α, S100β (B) in SCN; (C, D) Quantification of CD206+F4/80+ cell numbers (C) and TNF-α+ S100β+ area (D) in SCN; (E) Images of immunofluorescent staining of CD206, F4/80 in L4/5 DRG; (F) Quantification of CD206+F4/80+ cell numbers in L4/5 DRG. (G) IBA1 in the ipsilateral dorsal horn of L3/4 spinal cord; (H) IBA1+ cell numbers

in spinal cord after 7 days from partial sciatic nerve ligation (PSL) in the early phase model. Scale bar: 50 μm in (A, B and E) and 200 μm in (G). Student's t-test (n = 3, per group). Data represent the mean ± SD. *p < 0.05, **p < 0.01, ***p < 0.001.

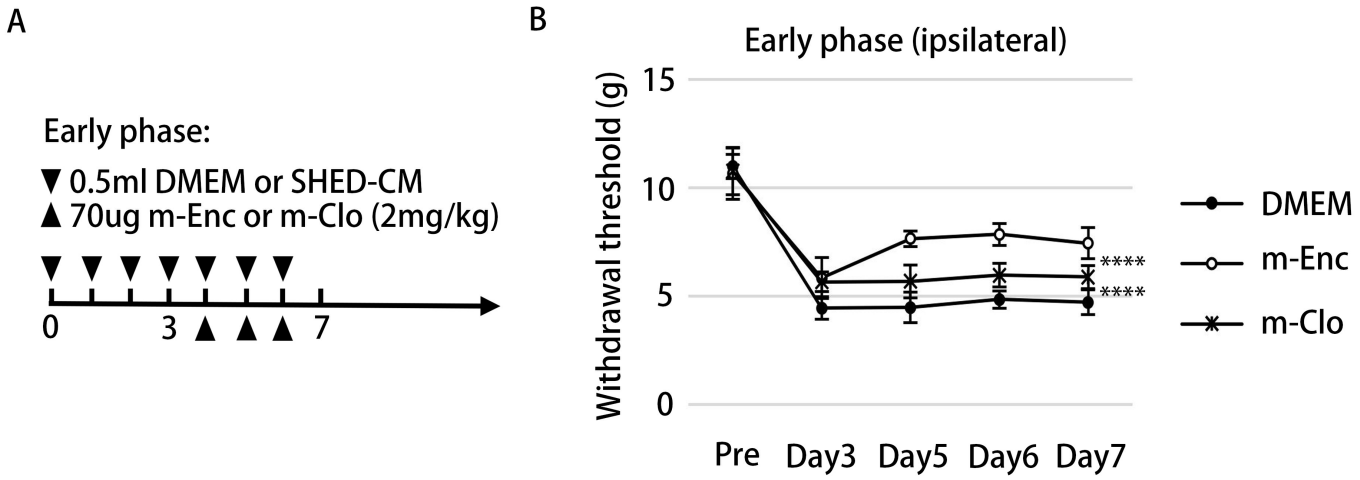


Figure 4

Effects of M2 depletion on SHED-CM-mediated behavioral recovery after partial sciatic nerve ligation (PSL). (A) Time course of M2 depletion in the early phase model. After PSL, mice were daily administered either 0.5 mL of SHED-CM or DMEM. From day 4 to 6, mannosylated-Clodrosome (m-Clo; for M2 depletion) or mannosylated-Encapsome (m-Enc; negative control) were injected together with SHED-CM. (B) The ipsilateral paw withdrawal thresholds. m-Clo, but not m-Enc, significantly inhibited the anti-nociceptive effects of SHED-CM. Notably, the paw withdrawal threshold in the m-Clo group was significantly higher than that in the DMEM group. ANOVA with Tukey's post-hoc test (n = 10, per group). Data represent the mean ± SD. ****p < 0.0001, for the m-Clo vs. m-Enc or DMEM comparisons.

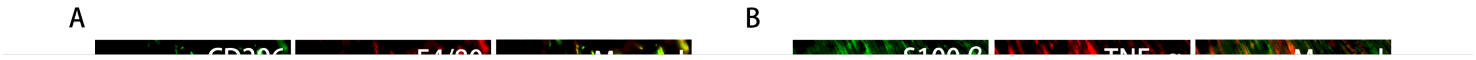


Figure 5

Effects of depletion of SHED-CM-induced M2 on the activation of Schwann cells and microglia. (A) Representative images of immunofluorescent staining of CD206, F4/80 (A) and TNF-α, S100β (B) in sciatic nerve (SCN); CD206, F4/80 in L4/5 DRG (C) and IBA1 in the ipsilateral dorsal horn of L3/4 spinal cord (D) after 7 days from the partial sciatic nerve ligation (PSL). Scale bar: 50 μm in (A, B and C), 200 μm in (D). (E-H) Quantification analysis of CD206+F4/80+ cell numbers (E) and TNF-α+ S100β+ area (F)

in SCN, CD206+ F4/80+ cell numbers in L4/5 dorsal root ganglion (DRG) (G) and IBA1+ cell numbers in spinal cord (H). Student's t-test (n = 3, per group). Data represent the mean ± SD. *p < 0.05, **p < 0.01, ***p < 0.001.

Figure 6

M2-CM suppresses the pro-nociceptive properties of TNF-α-activated Schwann cells in vitro. (A) Flow cytometry analysis of SHED-CM-induced M2 polarization. Mouse bone marrow-derived macrophages were treated with SHED-CM for 24 h and stained with F4/80 and CD206 antibodies. (B) qPCR analysis of human Schwann cells treated with TNF-α with or without M2-CM. Notably, M2-CM strongly inhibited the TNF-α-mediated elevation of pro-nociceptive factors and channels in Schwann cells. ANOVA with Tukey's post-hoc test (n = 3 per group). Data represent the mean ± SD; **p < 0.01, ****p < 0.0001.

Figure 7

Analgesic effect of M2-CM and MCP-1/sSiglec-9. (A) Time course of M2-CM treatment in the early phase model. (B) The ipsilateral paw withdrawal thresholds in the early phase model. Student's t-test (n = 10 in each group). (C) qPCR analysis of the sciatic nerves after 7 days from the partial sciatic nerve ligation (PSL) for the indicated mRNAs. Results are expressed relative to the levels in the sham-operated model. Student's t-test (n = 3, per group). (D) The immunofluorescent staining of IBA1 in the ipsilateral dorsal horn of the L3/4 spinal cord. Scale bar: 200 μm. (E): Quantitative analysis of the number of IBA1+ cells. Student's t-test (n = 3, per group). (F): Time course of MCP-1/sSiglec-9 treatment in the middle phase model. (G): The ipsilateral paw withdrawal thresholds in the middle phase model. ANOVA with Tukey's post-hoc test (n = 5 in each group). Data represent the mean ± SD; *, p < 0.05; **, p < 0.01; ****, p < 0.0001, for the M2-CM vs. DMEM or MCP-1/sSiglec-9 vs. PBS comparisons.

Supplementary Files

This is a list of supplementary files associated with this preprint. Click to download.

- Additionalfile1.pdf
- Additionalfile2supplementalfigure1.pdf
- Additionalfile3supplementalfigure2.pdf